Since January 2020 Elsevier has created a COVID-19 resource centre with free information in English and Mandarin on the novel coronavirus COVID-19. The COVID-19 resource centre is hosted on Elsevier Connect, the company's public news and information website.

Elsevier hereby grants permission to make all its COVID-19-related research that is available on the COVID-19 resource centre - including this research content - immediately available in PubMed Central and other publicly funded repositories, such as the WHO COVID database with rights for unrestricted research re-use and analyses in any form or by any means with acknowledgement of the original source. These permissions are granted for free by Elsevier for as long as the COVID-19 resource centre remains active.

Available online at www.sciencedirect.com
ScienceDirect
Mathematics and Computers in Simulation 205 (2023) 600–618
MATHEMATICS AND COMPUTERS IN SIMULATION
www.elsevier.com/locate/matcom

Original articles

Mathematical analysis of the impact of the media coverage in mitigating the outbreak of COVID-19

Ousmane Koutou[a,*], Abou Bakari Diabaté[b], Boureima Sangaré[b]

[a] *CUP-Kaya/Université Joseph KI-ZERBO, 01 BP 7021 Ouagadougou 01, Burkina Faso, Burkina Faso*
[b] *Département de mathématiques/Université Nazi BONI, 01 BP 1091 Bobo-Dioulasso 01, Burkina Faso*

Received 30 October 2021; received in revised form 25 August 2022; accepted 15 October 2022
Available online 22 October 2022

Abstract

In this paper, a mathematical model with a standard incidence rate is proposed to assess the role of media such as facebook, television, radio and tweeter in the mitigation of the outbreak of COVID-19. The basic reproduction number $\mathcal{R}_0$ which is the threshold dynamics parameter between the disappearance and the persistence of the disease has been calculated. And, it is obvious to see that it varies directly to the number of hospitalized people, asymptomatic, symptomatic carriers and the impact of media coverage. The local and the global stabilities of the model have also been investigated by using the Routh–Hurwitz criterion and the Lyapunov's functional technique, respectively. Furthermore, we have performed a local sensitivity analysis to assess the impact of any variation in each one of the model parameter on the threshold $\mathcal{R}_0$ and the course of the disease accordingly. We have also computed the approximative rate at which herd immunity will occur when any control measure is implemented. To finish, we have presented some numerical simulation results by using some available data from the literature to corroborate our theoretical findings.
© 2022 International Association for Mathematics and Computers in Simulation (IMACS). Published by Elsevier B.V. All rights reserved.

Keywords: COVID-19 mitigation; Media coverage; Mathematical study; Sensitivity analysis; Herd immunity; Numerical simulation

1. Introduction

COVID-19 is an infectious disease caused by a strain of coronavirus called SARS-CoV-2 which has led the whole world to a pandemic situation in such a short period of time. It is highly contagious with human-to-human transmission through out of respiratory droplets or contaminated surfaces. Symptoms of the disease are variable and as time passing, other variants have appeared. The most common signs are fever, coughing and difficulty in breathing which can cause acute respiratory distress that can lead to death. Appeared in November 2019 in Wuhan, mainland China, COVID-19 very quickly turned out to be a serious health problem around the world, with catastrophic consequences for the evolution of humankind. Our modern world has never been confronted with a disease of such magnitude [13,60]. Recent statistics of the course of the disease from its onset until September 2021, estimate that around 232 million people have been affected, of which more than 4.76 million have died [2,4]. The latency period of COVID-19 is up to two weeks and infected people can spread the virus even if they do not

* Corresponding author.
E-mail addresses: koutousman@gmail.com (O. Koutou), diaboubakre@gmail.com (A.B. Diabaté), mazou1979@yahoo.fr (B. Sangaré).

https://doi.org/10.1016/j.matcom.2022.10.017
0378-4754/© 2022 International Association for Mathematics and Computers in Simulation (IMACS). Published by Elsevier B.V. All rights reserved.

show symptoms of the disease [8,18,26]. The recommended measures for prevention are social distancing, wearing of masks in public, hand washing, mouth protection when sneezing or coughing. We can also list the disinfection of certain surfaces, the tracing of infected people and the quarantine of those exposed or showing the symptoms of the disease. Many types of vaccines are under development and vaccination campaigns are being implemented to counter the spread of the disease [6,24]. At the same time, work is underway to produce therapeutic drugs that could be efficacious against the virus. Meanwhile, the world is still shaken by the pandemic and to therefore control the quick spread of the disease, everywhere the authorities have responded by implementing lockdowns, travel restrictions by closing borders, etc [24,56,62]. The different measures taken to tackle the pandemic have provoked social and economic disruptions in many parts of the world. For instance, we have seen postponements, cancellations or to a lesser extent changes in the organization of many social events. The panic buying has led to supply shortages. In addition, agricultural disruptions have also caused food shortages [18,25]. Besides, many educational establishments have been partially or totally closed. Yet, this pandemic has had a positive impact on the environment such as the decrease in pollution [5,37,43].

The study of the novel coronavirus has relatively attracted some attention in mathematical epidemiology due to its seriousness and the way it has spread worldwide. Much work is underway to better understand the dynamics of disease transmission and to propose efficient strategies to control it spreading and all the related losses [2,8,13,41,50,65]. For instance, an interesting summary of several mathematical models that deal with some important aspects of COVID-19 is presented in Padmanabhan et al. [48]. Among the aspects of the disease dynamics that have received much attention and interest from the authors, we can point out the impact of the environment in Asamoah et al. [8], the impact of detection on COVID-19 transmission in Mushanyu et al. [43] and the impact of some public health measures in Cotta et al. [15]. Demongeot et al. [16] wrote an article devoted to identifying parameters in the SI model of COVID-19. A real-time surveillance and evaluation with a second derivative model in the first two months of COVID-19 epidemic in China has been proposed by Chen et al. [13]. Moreover, the work of Z. Liu et al. [38] has helped to predict the cumulaive number of cases for the COVID-19 epidemic in China from early data. Kassa et al. [25,26] and Obsu et al. [46] analyzed the relevance of the different strategies used to control the spread of the disease. In addition, the role of asymptomatic people, quarantine, isolation and the use of face mask has been investigated by Ivorra et al. [24], Ali et al. [4], Zeb et al. [62] and Eikenberry et al. [18], respectively. In contemporary times, media coverage is identified as an alternate control measure which brings behavioral changes among susceptible individuals, and it can be seen as partial treatment at low cost. Thus, several authors have proposed some mathematical models to investigate the effect of media coverage in the control of COVID-19 among which we can list Feng et al. [19], Kumar et al. [33], Rai et al. [49], Yan et al. [59], Zhou et al. [63].

Furthermore, one of the major issues public health policy-makers meet in the implementation of any strategy for COVID-19 control is public adherence due to people's perceived beliefs. To raise awareness in these uncertain times, one of the priorities of the world's media was to cover the pandemic. But the ever-changing and sometimes unverified nature of the published data on the ongoing of the disease has left journalists and researchers with difficulty to provide accurate information to the public [28,31,54]. Also, since it is a global disease, COVID-19 is called an infodemic. For example, direct access to information through platforms such as Facebook, Twitter and Youtube makes users vulnerable to rumors and questionable information [8,37,46]. And even though a lot of misinformation have circulated through social media and mass media, in general the use of social media led to behavioral changes and therefore made government measures more effective against the rapid spread of the virus [11,46]. Some platforms have also been used by political movements and public health organizations to effectively disseminate information and reach as many people as possible [18,25,37]. It is therefore evident that media coverage has had a great influence on the disease dynamics. In the light of that, we hereby consider the impact of the media in the mitigation of the epidemic [11,23,37]. For that, we built a compartmental mathematical model by considering a standard incidence function in which we consider the contribution of asymptomatic, hospitalized and symptomatic people, the loss of immunity even though this aspect about the COVID-19 is not yet well understood, and mainly the introduction of the parameter M accounting for the media (facebook, television, radio, tweeter) coverage that led to new habits and more seriousness in applying self-protective measures.

After the statement of the problem, we organize the remaining part of the paper as follows. In Section 2, we explain the different steps and assumptions upon which we have built our model, we present our compartment diagram and our disease transmission model. Section 3 concerns the mathematical study of the proposed model.

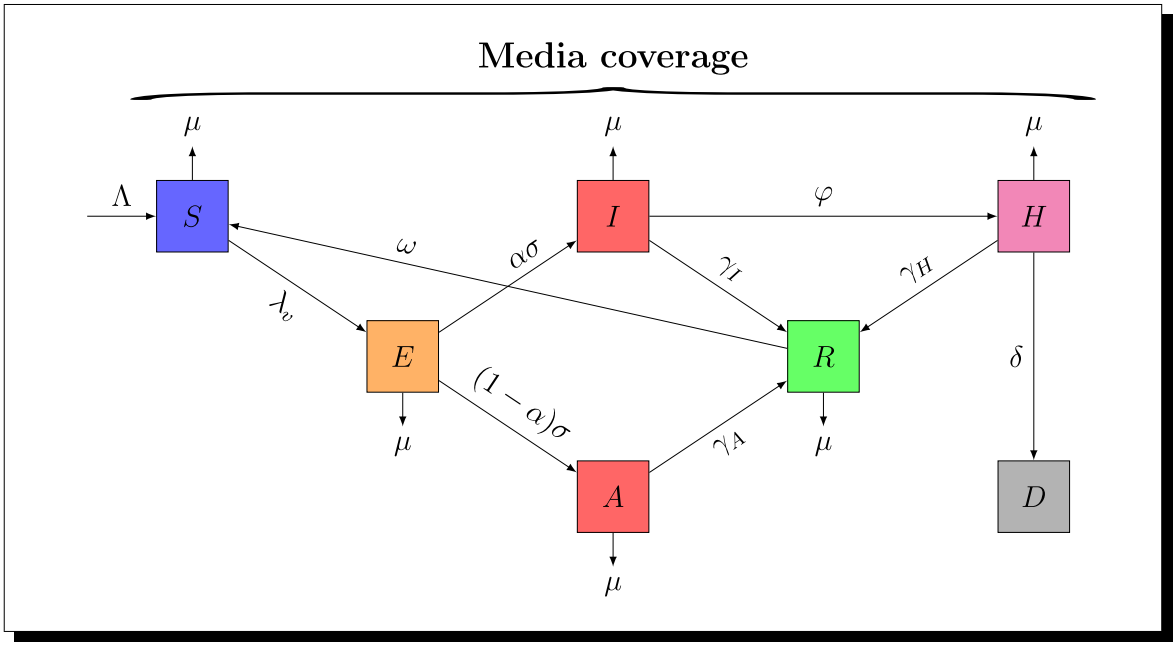

Fig. 1. Compartmental representation of the disease transmission dynamics.

More precisely, in this section, we proved the well-posedness of the model, we computed the disease-free equilibrium point and the basic reproduction number that has been shown to be the key threshold parameter in investigating the disease dynamics. Moreover, thanks to certain conditions on $\mathcal{R}_0$ ($\mathcal{R}_0 < 1$ or $\mathcal{R}_0 > 1$), to the Routh–Hurwitz criterion and to Lyapunov's function principle [29,30,32], we have studied the local and global stabilities of the steady states. The sensitivity of $\mathcal{R}_0$ to the various parameters that compose it and herd immunity were studied in Section 4. We devoted Section 5 to the numerical simulations. The paper ends with a conclusion section where we give recommendations and perspectives.

2. Model formulation

A deterministic model of COVID-19 global behavior is hereby presented. The population under consideration is split into several compartments. We then consider Susceptible $S(t)$, Exposed $E(t)$, Asymptomatic infectious $A(t)$, Symptomatic infectious $I(t)$, Hospitalized $H(t)$ and Recovered individuals $R(t)$; we also consider a compartment $D(t)$ that tracks cumulative deaths due to the disease after hospitalization [18]. Therefore, at any time $N(t) = S(t) + E(t) + A(t) + I(t) + H(t) + R(t)$ is the total size of human population [1]. In addition, β is the baseline transmission rate, η_1 and η_2 account for the relative infectivity potential of hospitalized and asymptomatic carriers. σ is the rate at which an exposed individual moves to the infectious class where individuals show symptoms of the disease and α is the proportion of cases that goes to the symptomatic class after the latency period. We assume that only symptomatic people are hospitalized and the rate of hospitalization is φ. However, besides the natural death rate μ of the human population, there is the COVID-induced death rate denoted by δ. γ_A, γ_I and γ_H are the recovery rates of asymptomatic, symptomatic and hospitalized individuals, respectively. Besides, ω is the losing immunity rate. The inflow of individuals into the population is assumed to enter the susceptible compartment at the rate Λ (i.e recruitment rate which comprises new births and immigrants) [8,18,60].

We choose a standard incidence function as the force of new infection given by the following quantity

$$\lambda_v = (1 - M)\beta \frac{\eta_1 H + \eta_2 A + I}{N} \tag{1}$$

with $M = f + m_{tv} + r + Tw$ where f is the efficiency rate of information shared through facebook, m_{tv} is the efficiency rate of information shared on television, r is the efficiency rate of information shared through radio and

Tw is the efficiency rate of information shared on tweeter [42]. Indeed, the parameter M, represents the rate of efficiency of the media coverage within the community. It should be noted that the media coverage efficiency rate M hardly reaches 1 ($M < 1$). In other words, it is very difficult that the impact of the media coverage in the behavior change reaches 100% [33,42,49,58,63]; this is because human behavior is very unpredictable. In fact, the advisable changes in behavior relates to community habits and therefore the implementation is much more difficult for most people. Lot of people understand, accept, incorporate and implement barrier measures after several media campaigns. We can add to this the exorbitant cost of the media coverage, the decrease of media coverage impact as time passing, the lack of knowledge about certain aspects of the COVID-19 disease dynamics. In general, other control methods are then added to media awareness work in order to achieve a rapid extinction of the disease [33,42,49,58,63]. In this work, one of our objectives is to approximate a minimum value of M from which an extinction of the COVID-19 disease is possible in an adequate environment. Moreover, the overall dynamics described above can be summarized by the following diagram of Fig. 1.

Otherwise, the disease transmission dynamics is then given by the following system

$$\begin{cases} \dot{S}(t) = \Lambda + \omega R - (1-M)\beta \dfrac{\eta_1 H + \eta_2 A + I}{N} S - \mu S, \\ \dot{E}(t) = (1-M)\beta \dfrac{\eta_1 H + \eta_2 A + I}{N} S - (\sigma + \mu) E \\ \dot{I}(t) = \alpha\sigma E - (\varphi + \gamma_I + \mu) I, \\ \dot{A}(t) = (1-\alpha)\sigma E - (\gamma_A + \mu) A, \\ \dot{H}(t) = \varphi I - (\delta + \gamma_H + \mu) H, \\ \dot{R}(t) = \gamma_I I + \gamma_A A + \gamma_H H - (\omega + \mu) R \\ \dot{D}(t) = \delta H. \end{cases} \tag{2}$$

with the following nonnegative initial conditions $S(0) = S_0 > 0$, $E(0) = E_0 > 0$, $A(0) = A_0 > 0$, $I(0) = I_0 > 0$, $H(0) = H_0 > 0$ and $R(0) = R_0 > 0$, [1,22,27,47].

3. Mathematical investigation of our model

3.1. Positivity and boundedness properties

Theorem 3.1. *If S_0, E_0, A_0, I_0, H_0, R_0 are nonnegative, then so are $S(t)$, $E(t)$, $A(t)$, $I(t)$, $H(t)$, $R(t)$ for all time $t > 0$. Moreover, $\limsup_{t\to+\infty} N(t) \leq \dfrac{\Lambda}{\mu}$.*

Proof. For that, we first show by using the contradiction that the state variable S is nonnegative for all $t \geq 0$. Let $e(t) = \min\{S(t), E(t), A(t), I(t), H(t), R(t)\}$ and suppose that there exists $t_1 > 0$ such that $e(t_1) = 0$ and $e(t) > 0$ for all $t \in (0, t_1)$. Therefore, if $e(t) = S(t)$ then each state of model (2) is positive and from the first equation of (2), we have

$$\dot{S}(t) > -\mu S(t). \tag{3}$$

It then follows that

$$0 = S(t_1) > S_0 \exp(-\mu t_1) > 0 \tag{4}$$

which leads to a contradiction.

Similar proof can be given for the other state variables. Thus, any solution of system (2) is nonnegative for $t \geq 0$.

Moreover, the total number of the population $N(t)$ at any time is governed by

$$\dot{N}(t) = \Lambda - \mu N(t) - \delta H. \tag{5}$$

Thus, for the initial conditions $0 \leq N(0) \leq \frac{\Lambda}{\mu}$, by using Gronwall inequality [10,32], we get

$$0 \leq N(t) \leq \frac{\Lambda}{\mu}. \tag{6}$$

Hence, system (2) defines a dynamical on

$$\Omega = \left\{ (S(t), E(t), A(t), I(t), H(t), R(t)) \in \mathbb{R}^5 \middle| \ 0 \leq N(t) \leq \frac{\Lambda}{\mu} \right\}. \quad \square$$

3.2. Basic reproduction number and no-disease steady state stability

3.2.1. Basic reproduction number

To compute the equilibrium solutions, we set the right-hand-side of system (2) to zero. We then obtain the disease-free equilibrium as follows

$$\mathcal{E}_0 = \left(\frac{\Lambda}{\mu}, 0, 0, 0, 0 \right). \tag{7}$$

The basic reproduction number which is a key value to analyzing the threshold dynamics of the model is calculated by using the well-known method of the next-generation matrix given in [17,57]. Adopting the notation $X = (E, I, A, H)$ for the infected states of model (2), we obtain the following vector functions

$$\mathcal{F}(X) = \begin{pmatrix} (1-M)\beta \dfrac{\eta_1 H + \eta_2 A + I}{N} S \\ 0 \\ 0 \\ 0 \end{pmatrix} \text{ and } \mathcal{V}(X) = \begin{pmatrix} -(\sigma+\mu)E \\ \alpha\sigma E - (\varphi + \gamma_I + \mu)I, \\ (1-\alpha)\sigma E - (\gamma_A + \mu)A, \\ \varphi I - (\delta + \gamma_H + \mu)H \end{pmatrix}.$$

The next-generation matrix is $J_{\mathcal{F}}(\mathcal{E}_0)\left(J_{\mathcal{V}}(\mathcal{E}_0)\right)^{-1}$ where

$$J_{\mathcal{F}}(\mathcal{E}_0) = \begin{pmatrix} 0 & (1-M)\beta & (1-M)\beta\eta_2 & (1-M)\beta\eta_1 \\ 0 & 0 & 0 & 0 \\ 0 & 0 & 0 & 0 \\ 0 & 0 & 0 & 0 \end{pmatrix}$$

and

$$J_{\mathcal{V}}(\mathcal{E}_0) = \begin{pmatrix} -(\sigma+\mu) & 0 & 0 & 0 \\ \alpha\sigma & -(\varphi+\gamma_I+\mu) & 0 & 0 \\ (1-\alpha)\sigma & 0 & -(\gamma_A+\mu) & 0 \\ 0 & \varphi & 0 & -(\delta+\gamma_H+\mu) \end{pmatrix}.$$

The basic reproduction number denoted by $\mathcal{R}_0$ is the average number of secondary cases induced by an infected individual during his/her entire period of infectiousness in a wholly susceptible population [17,31,54,57]. In the mathematical framework, $\mathcal{R}_0$ can be defined as the spectral radius of $J_{\mathcal{F}}(\mathcal{E}_0)\left(J_{\mathcal{V}}(\mathcal{E}_0)\right)^{-1}$.

Therefore,

$$\mathcal{R}_0 = \mathcal{R}_I + \mathcal{R}_A + \mathcal{R}_H \tag{8}$$

where

$$\mathcal{R}_I = \frac{(1-M)\beta\alpha\sigma}{(\sigma+\mu)(\varphi+\gamma_I+\mu)},$$
$$\mathcal{R}_A = \frac{(1-M)\beta\eta_2(1-\alpha)\sigma}{(\sigma+\mu)(\gamma_A+\mu)},$$
$$\mathcal{R}_H = \frac{(1-M)\beta\eta_1\alpha\sigma\varphi}{(\sigma+\mu)(\varphi+\gamma_I+\mu)(\delta+\gamma_H+\mu)}.$$

Furthermore, $\mathcal{R}_I$, $\mathcal{R}_A$ and $\mathcal{R}_H$ are the secondary infection numbers seeded through direct contact by the infectious individuals I, the asymptomatic carriers A, and the hospitalized people H, respectively [7,8,31].

3.2.2. Local and global stability analysis of $\mathcal{E}_0$

The forthcoming result is a direct application of Theorem 2 in [57].

Theorem 3.2. *For $\mathcal{R}_0 < 1$, $\mathcal{E}_0$ is locally asymptotically stable and unstable if $\mathcal{R}_0 > 1$.*

Proof. When we consider the infected states (E, I, A, H) and then linearizing model (2) about $\mathcal{E}_0$, yields

$$\mathbb{B}_0 = \begin{pmatrix} -(\sigma+\mu) & (1-M)\beta & (1-M)\beta\eta_2 & (1-M)\beta\eta_1 \\ \alpha\sigma & -(\varphi+\gamma_I+\mu) & 0 & 0 \\ (1-\alpha)\sigma & 0 & -(\gamma_A+\mu) & 0 \\ 0 & \varphi & 0 & -(\delta+\gamma_H+\mu) \end{pmatrix}.$$

Setting $b_1 = \sigma+\mu$, $b_2 = \varphi+\gamma_I+\mu$, $b_3 = \gamma_A+\mu$, $b_4 = \delta+\gamma_H+\mu$ and considering an eigenvalue λ of the matrix $\mathbb{B}_0$, we then compute the characteristic polynomial as follows

$$P(\lambda) = \det(\mathbb{B}_0 - \lambda I_4) = \det\begin{pmatrix} -(b_1+\lambda) & (1-M)\beta & (1-M)\beta\eta_2 & (1-M)\beta\eta_1 \\ \alpha\sigma & -(b_2+\lambda) & 0 & 0 \\ (1-\alpha)\sigma & 0 & -(b_3+\lambda) & 0 \\ 0 & \varphi & 0 & -(b_4+\lambda) \end{pmatrix}.$$

Consequently,

$$P(\lambda) = d_0\lambda^4 + d_1\lambda^3 + d_2\lambda^2 + d_3\lambda + d_4$$

where,

$$\begin{aligned}
d_0 &= 1,\\
d_1 &= b_1+b_2+b_3+b_4 > 0,\\
d_2 &= b_1b_2(1-\mathcal{R}_I) + b_1b_3(1-\mathcal{R}_A) + b_1b_4 + b_2b_3 + b_2b_4 + b_3b_4 > 0,\\
d_3 &= b_1b_2(b_3+b_4)(1-\mathcal{R}_0) + b_1b_3b_4(1-\mathcal{R}_A) + b_2b_3b_4 + \frac{(1-M)\beta\eta_1\alpha\sigma\varphi b_3}{b_4}\\
&\quad + \frac{(1-M)\beta\eta_2(1-\alpha)\sigma b_2b_4}{b_3} > 0,\\
d_4 &= b_1b_2b_3b_4(1-\mathcal{R}_0) > 0.
\end{aligned}$$

Moreover, referring to the Routh–Hurwitz criterion, it then follows that:

$$\begin{aligned}
\Delta_1 &= d_1d_2 - d_0d_3\\
&= b_1d_2 + b_1b_2^2(1-\mathcal{R}_I) + b_1b_3^2(1-\mathcal{R}_A) + (1-M)\beta\eta_1\alpha\sigma\varphi\\
&\quad + (b_2+b_4)(b_3^2 + b_1b_3 + b_1b_4 + b_2b_3 + b_2b_4 + b_3b_4) > 0,\\
\Delta_2 &= d_3\Delta_1 - d_1^2d_4\\
&= b_1b_2(b_3+b_4)(1-\mathcal{R}_0)[b_1b_2(b_1+b_2)(1-\mathcal{R}_I) + b_1b_3(b_1+b_3)(1-\mathcal{R}_A) + b_2^2b_3\\
&\quad + b_2b_3^2 + b_4^2(b_1+b_2) + 2b_1b_2b_3 + (1-M)\beta\alpha\sigma] + b_1b_2b_4^2(1-\mathcal{R}_0)(b_1+b_2)^2\\
&\quad + \left(b_1b_3b_4(1-\mathcal{R}_A) + b_2b_3b_4 + \frac{(1-M)\beta\eta_2(1-\alpha)\sigma b_2b_4}{b_3} + \frac{(1-M)\beta\eta_1\alpha\sigma\varphi b_3}{b_4}\right)\Delta_1 > 0.
\end{aligned}$$

From above, since $\Delta_1 = d_1d_2 - d_0d_3 > 0$ and $\Delta_2 = d_3\Delta_1 - d_1^2d_4 > 0$ then the disease-free equilibrium point of the model (2) is locally asymptotically stable [32,52]. □

Now, let us investigate the global stability results of the no-disease equilibrium point.

Theorem 3.3. *If $\mathcal{R}_0 < 1$ then $\mathcal{E}_0$ is globally asymptotically stable.*

Proof. For the demonstration of the above statement, we use the Lyapunov's functional technique. Therefore, we consider this Lyapunov candidate [21,29]

$$L = E + \left(\frac{(1-M)\beta}{b_2} + \frac{(1-M)\beta\eta_1\varphi}{b_2 b_4}\right) I + \frac{(1-M)\beta\eta_2}{b_3} A + \frac{(1-M)\beta\eta_1}{b_4} H.$$

It is obvious to see that the functional L is equal to zero at the empty disease equilibrium point $\mathcal{E}_0$ and positive elsewhere. However, by computing the derivative of the Lyapunov functional L and substituting $\dot{E}$, $\dot{I}$, $\dot{A}$, and $\dot{H}$ we obtain

$$\begin{aligned}
\dot{L} &= \left((1-M)\beta\frac{\eta_1 H + \eta_2 A + I}{N} S - b_1 E\right) + \left(\frac{(1-M)\beta}{b_2} + \frac{(1-M)\beta\eta_1\varphi}{b_2 b_4}\right)(\alpha\sigma E - b_2 I) \\
&+ \frac{(1-M)\beta\eta_2}{b_3}((1-\alpha)\sigma E - b_3 A) + \frac{(1-M)\beta\eta_1\varphi}{b_4}(\varphi I - b_4 H) \\
&= \left((1-M)\beta\eta_1\frac{S}{N} - b_4 \times \frac{(1-M)\beta\eta_1\varphi}{b_4}\right) H + \left((1-M)\beta\eta_2\frac{S}{N} - b_3 \times \frac{(1-M)\beta\eta_2}{b_3}\right) A \\
&+ \left((1-M)\beta\frac{S}{N} - \frac{(1-M)\beta b_2}{b_2} - \frac{(1-M)\beta\eta_1\varphi b_2}{b_2 b_4} + \frac{(1-M)\beta\eta_1\varphi}{b_4}\right) I \\
&+ \left(-b_1 + \frac{(1-M)\beta\alpha\sigma}{b_2} + \frac{(1-M)\beta\eta_1\varphi\alpha\sigma}{b_2 b_4} + \frac{(1-M)\beta\eta_2(1-\alpha)\sigma}{b_3}\right) E.
\end{aligned}$$

Noticing that $\dfrac{S}{N} \leq 1$, it then follows that

$$\dot{L} \leq b_1(\mathcal{R}_0 - 1)E.$$

Consequently, $\dot{L} \leq 0$ whenever $\mathcal{R}_0 < 1$. Furthermore, $\dot{L} = 0$ if and only if $E = I = A = H = 0$. So, the invariant associated with the infected states of system (2) is defined as

$$\zeta = \left\{x = (E, I, A, H) \in \mathbb{R}^4 : \dot{L}(x) = 0\right\}.$$

Thus, by the Krasovskii–LaSalle theorem, since the set ζ contains only the disease-free equilibrium $\mathcal{E}_0$ then $\mathcal{E}_0$ is globally asymptotically stable whenever $\mathcal{R}_0 < 1$ [34,35]. □

3.3. Computation of the endemic steady-state $\mathcal{E}^*$

3.3.1. Existence of $\mathcal{E}^*$

Theorem 3.4. *System (2) admits a unique positive endemic equilibrium* $\mathcal{E}^* = (S^*, E^*, I^*, A^*, H^*, R^*)$ *whenever* $\mathcal{R}_0 > 1$.

Proof. By putting the right hand side of system (2) to zero, and keeping each state variable different from zero ($S \neq 0$, $E \neq 0$, $I \neq 0$, $A \neq 0$, $H \neq 0$ and $R \neq 0$) then one obtains

$$S^* = \frac{b_4\Lambda - \delta\varphi I^*}{\mu b_4 \mathcal{R}_0},\quad E^* = \frac{b_2}{\alpha\sigma} I^*,\quad A^* = \frac{(1-\alpha)b_2}{\alpha b_3} I^*,\quad H^* = \frac{\varphi}{b_4} I^*$$

$$R^* = \frac{\alpha\gamma_I b_3 b_4 + (1-\alpha)\gamma_A b_2 b_4 + \alpha\varphi\gamma_H b_3}{\alpha(\omega+\mu)b_3 b_4} I^*$$

and

$$I^* = \frac{\alpha(\omega+\mu)b_3 b_4 \Lambda(\mathcal{R}_0 - 1)}{\alpha b_3 b_4 \mathcal{Q}_1 + (1-\alpha)b_2 b_4 \mathcal{Q}_2 + \alpha\varphi b_3 \mathcal{Q}_3},$$

with

$$\begin{aligned}
\mathcal{Q}_1 &= (1-M)\beta(\omega+\mu) - \omega\gamma_I\mathcal{R}_0, \\
\mathcal{Q}_2 &= (1-M)\beta\eta_2(\omega+\mu) - \omega\gamma_A\mathcal{R}_0, \\
\mathcal{Q}_3 &= ((1-M)\beta\eta_1 - \delta)(\omega+\mu) - \omega\gamma_H\mathcal{R}_0.
\end{aligned}$$

It is obvious that $\mathcal{R}_0 = 1$ leads to the disease-free equilibrium, whereas when $\mathcal{R}_0 > 1$ then there exists a unique endemic equilibrium. □

3.3.2. Local and global stability of $\mathcal{E}^*$

Theorem 3.5. *If $\mathcal{R}_0 > 1$, then the endemic steady-state $\mathcal{E}^*$ is locally asymptotically stable.*

Proof. Indeed, the linearization of model (2) about the endemic equilibrium point gives

$$\mathbb{B}_1 = \begin{pmatrix} -b_1 - C & \dfrac{(1-M)\beta}{\mathcal{R}_0} - C & \dfrac{(1-M)\beta\eta_2}{\mathcal{R}_0} - C & \dfrac{(1-M)\beta\eta_1}{\mathcal{R}_0} - C \\ \alpha\sigma & -b_2 & 0 & 0 \\ (1-\alpha)\sigma & 0 & -b_3 & 0 \\ 0 & \varphi & 0 & -b_4 \end{pmatrix},$$

where

$$C = \frac{\mu b_1 b_2 b_4 I^*}{\alpha\sigma(b_4\Lambda - \delta\varphi I^*)}.$$

Therefore, the characteristic polynomial is given by

$$Q(\lambda) = \begin{vmatrix} -(b_1+\lambda) - C & \dfrac{(1-M)\beta}{\mathcal{R}_0} - C & \dfrac{(1-M)\beta\eta_2}{\mathcal{R}_0} - C & \dfrac{(1-M)\beta\eta_1}{\mathcal{R}_0} - C \\ \alpha\sigma & -(b_2+\lambda) & 0 & 0 \\ (1-\alpha)\sigma & 0 & -(b_3+\lambda) & 0 \\ 0 & \varphi & 0 & -(b_4+\lambda) \end{vmatrix}.$$

And then,

$$Q(\lambda) = D_0\lambda^4 + D_1\lambda^3 + D_2\lambda^2 + D_3\lambda + D_4$$

with,

$$\begin{aligned}
D_0 &= 1,\\
D_1 &= b_1 + b_2 + b_3 + b_4 + C > d_1 > 0,\\
D_2 &= b_1b_2\left(1 - \frac{\mathcal{R}_I}{\mathcal{R}_0}\right) + b_1b_3\left(1 - \frac{\mathcal{R}_A}{\mathcal{R}_0}\right) + b_1b_4 + b_2b_3 + b_2b_4 + b_3b_4 + (b_2+b_3+b_4)C + \alpha\sigma C\\
&\quad + (1-\alpha)\sigma C > d_2 > 0,\\
D_3 &= b_1b_3b_4\left(1 - \frac{\mathcal{R}_A}{\mathcal{R}_0}\right) + b_2b_3b_4 + \frac{(1-M)\beta\eta_1\alpha\sigma\varphi b_3}{b_4\mathcal{R}_0} + \frac{(1-M)\beta\eta_2(1-\alpha)\sigma b_2b_4}{b_3\mathcal{R}_0}\\
&\quad + (b_2b_3 + b_2b_4 + b_3b_4)C + \alpha\sigma(b_3+b_4)C + (1-\alpha)\sigma(b_2+b_4)C + \alpha\sigma C > 0,\\
D_4 &= b_2b_3b_4C + \alpha\sigma b_3b_4C + (1-\alpha)\sigma b_2b_4C + \alpha\sigma\varphi C b_3 > 0.
\end{aligned}$$

Furthermore,

$$\begin{aligned}
\Delta_1' &= D_1D_2 - D_0D_3\\
&= b_1D_2 + b_1b_2^2\left(1 - \frac{\mathcal{R}_I}{\mathcal{R}_0}\right) + b_1b_3^2\left(1 - \frac{\mathcal{R}_A}{\mathcal{R}_0}\right) + \frac{(1-M)\beta\eta_1\alpha\sigma\varphi}{\mathcal{R}_0}\\
&\quad + (b_2+b_4)(b_3^2 + b_1b_3 + b_1b_4 + b_2b_3 + b_2b_4 + b_3b_4)\\
&\quad + \left(b_2^2 + b_2b_3 + b_2b_4 + b_3^2 + b_3b_4 + b_4^2 + \alpha\sigma\,(\gamma_I + \mu) + (1-\alpha)\sigma b_3 + D_2\right)C > 0
\end{aligned}$$

and

$$\begin{aligned}
\Delta_2' &= D_3\Delta_1' - D_1^2D_4\\
&= [b_1b_2(2b_2b_3^2 + b_1b_4^2 + 2b_2b_3b_4 + 2b_2b_4^2 + b_3b_4^2 + b_4^2) + b_2^2b_3(b_3^2 + b_4^2 + b_2b_3 + b_2b_4 + b_3b_4)\\
&\quad + b_2^2b_4^2(b_2+b_4) + b_3b_4(2b_1b_2 + b_2^2) + b_4^2(b_1b_2 + b_1b_3 + b_1b_4 + b_2b_3) + \alpha\sigma b_4^2(b_1^2 + b_2^2 + b_1b_2 + b_2b_4)\\
&\quad + (1-\alpha)\sigma(2b_1b_2^2b_3 + b_1^2b_2^2 + b_2^2b_3^2 + b_2^3b_3 + b_1b_3b_4^2 + b_2b_3^2b_4 + b_3b_4^3 + b_3^2b_4^2) + \alpha\sigma\varphi(b_1^2b_4 + b_1b_4^2$$

$$
\begin{aligned}
&+ b_2^2b_4 + b_2b_4^2 + 2b_1b_2b_4) + \alpha\sigma(\gamma_I + \mu)(b_3^3 + 2b_1b_3^2 + b_2b_3^2 + b_3^2b_4) - \alpha\sigma\varphi b_1^2b_3]C + [b_1b_2(b_3^2 + 2b_4^2\\
&+ b_2b_3 + b_2b_4 + b_3b_4 + b_3 + 2b_4) + b_2b_3(b_2^2 + b_3^2 + b_4^2 + 2b_2b_3 + 2b_2b_4 + b_3b_4 + b_2 + 2b_4) + b_2b_4^2\\
&+ b_2^2b_4(1 + b_2 + 2b_4) + (b_3b_4 + b_1b_4)(b_3 + b_4) + b_4^3 + \alpha\sigma(b_3^3 + b_2^2b_4 + b_2b_4^2 + b_1b_3^2 + \sigma b_1b_3 + \sigma b_1b_4)\\
&+ (1-\alpha)\sigma(b_1b_2b_3 + b_1b_2^2 + b_2^3 + b_2b_3b_4 + b_3b_4^2 + \alpha\sigma b_3^2 + \sigma b_3b_4 + \sigma b_1b_2 + \sigma b_1b_4 + (1-\alpha)\sigma b_2b_3)\\
&+ \alpha\sigma\varphi(b_1b_2 + 2b_1b_4 + b_2^2 + b_4^2 + b_2b_4 + \sigma b_1 + (1-\alpha)\sigma b_3)]C^2 + [b_2b_3(2 + b_2 + b_3 + b_4) + b_3b_4\\
&+ b_2b_4(2 + b_2 + b_4) + b_4^2 + \alpha\sigma(b_3^2 + \sigma(b_2 + b_3 + b_4)) + (1-\alpha)\sigma(b_2^2 + \sigma b_4) + \alpha\sigma\varphi(b_2 + b_4 + \sigma)]C^3\\
&+ \left[b_1b_3b_4\left(1 - \frac{\mathcal{R}_A}{\mathcal{R}_0}\right) + b_2b_3b_4 + b_3b_4C + \frac{(1-M)\beta\eta_2(1-\alpha)\sigma b_2b_4}{b_3\mathcal{R}_0} + \frac{(1-M)\beta\eta_1\alpha\sigma\varphi b_3}{b_4\mathcal{R}_0}\right]\Delta_1'\\
&+ \left[b_1b_2\,(b_1 + b_2 + C)\left(1 - \frac{\mathcal{R}_I}{\mathcal{R}_0}\right) + b_1b_3\,(b_1 + b_3 + C)\left(1 - \frac{\mathcal{R}_A}{\mathcal{R}_0}\right) + \frac{(1-M)\beta\eta_1\alpha\sigma\varphi}{\mathcal{R}_0}\right]((b_2C\\
&+ \alpha\sigma C)(b_3 + b_4) + (1-\alpha)\sigma C(b_2 + b_4) + \alpha\sigma\varphi C) > 0.
\end{aligned}
$$

Then, using Routh–Hurwitz criterion, all the eigenvalues of the Jacobian matrix have negative real parts. Thus, the endemic equilibrium point $\mathcal{E}^*$ is locally asymptotically stable [39,44]. □

In the following paragraph, we seek to investigate the global stability of $\mathcal{E}^*$. For that, we need to find a suitable Lyapunov function.

Theorem 3.6. *Let $\mathcal{R}_0 > 1$. Whenever $sign(N - N^*) = sign(H - H^*)$, the endemic equilibrium $\mathcal{E}^*$ of model (2) is globally asymptotically stable.*

Proof. With the following Lyapunov candidate [14,29]

$$
\begin{aligned}
\dot{\mathcal{V}} &= \left(S - S^*\right) + \left(E - E^*\right) + \left(I - I^*\right) + \left(A - A^*\right) + \left(H - H^*\right) + \left(R - R^*\right)\\
&\quad - \left(S^* + E^* + I^* + A^* + H^* + R^*\right)\ln\left(\frac{S + E + I + A + H + R}{S^* + E^* + I^* + A^* + H^* + R^*}\right),
\end{aligned}
$$

one can easily check that the above function is zero at the endemic equilibrium and positive elsewhere. Moreover, it can also be rewritten as follows:

$$
\mathcal{V} = N - N^* - N^*\ln\frac{N}{N^*}.
$$

Therefore, the derivative form of the function $\mathcal{V}$ is given as

$$
\begin{aligned}
\dot{\mathcal{V}} &= \left(1 - \frac{N^*}{N}\right)\dot{N}\\
&= \left(1 - \frac{N^*}{N}\right)(\Lambda - \mu N - \delta H)\\
&= \frac{N - N^*}{N}\left(\mu N^* + \delta H^* - \mu N - \delta H\right)\\
&= \frac{N - N^*}{N}\left[-\mu(N - N^*) - \delta(H - H^*)\right]\\
&= -\frac{(N - N^*)^2}{N} - \frac{\delta(N - N^*)(H - H^*)}{N}\\
&\leq 0.
\end{aligned}
$$

Consequently, thanks to LaSalle's invariance principle, the solution $\mathcal{E}^*$ is said to be globally asymptomatically stable [34,35]. □

4. Sensitivity analysis and herd immunity

4.1. Sensitivity analysis

Performing a sensitivity analysis helps us to understand how changes in the model parameters will affect the disease spreading dynamics [8,39]. And to carry it out, a simple approach is used to calculate the sensitivity index

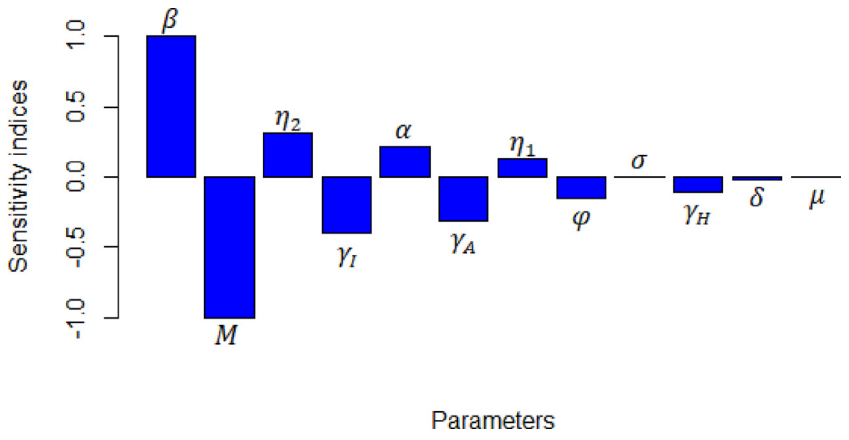

Fig. 2. Sensitivity indices diagram for $\mathcal{R}_0$.

of each parameter that appeared in $\mathcal{R}_0$ through out of the following formula [7,45]:

$$\chi_p^{\mathcal{R}_0} = \frac{\partial \mathcal{R}_0}{\partial p} \times \frac{p}{\mathcal{R}_0} \simeq \frac{\%\Delta \mathcal{R}_0}{\%\Delta p}.$$

Therefore,

$$\chi_\beta^{\mathcal{R}_0} = 1,\ \chi_M^{\mathcal{R}_0} = -\frac{M}{1-M},\ \chi_\sigma^{\mathcal{R}_0} = 1 - \frac{\sigma}{b_1},\ \chi_\alpha^{\mathcal{R}_0} = \frac{\alpha\,(b_3b_4 - \eta_2 b_2 b_4 + \eta_1\varphi b_3)}{\alpha b_3 b_4 + \eta_2(1-\alpha)b_2b_4 + \eta_1\alpha\varphi b_3},$$

$$\chi_{\eta_1}^{\mathcal{R}_0} = \frac{\eta_1\alpha\varphi b_3}{\alpha b_3 b_4 + \eta_2(1-\alpha)b_2b_4 + \eta_1\alpha\varphi b_3},\ \chi_{\gamma_I}^{\mathcal{R}_0} = -\frac{\gamma_I\,(\alpha b_3 b_4 + \eta_1\alpha\varphi b_3)}{b_2\,(\alpha b_3 b_4 + \eta_2(1-\alpha)b_2b_4 + \eta_1\alpha\varphi b_3)},$$

$$\chi_{\gamma_A}^{\mathcal{R}_0} = -\frac{\gamma_A\eta_2(1-\alpha)b_2b_4}{b_3\,(\alpha b_3 b_4 + \eta_2(1-\alpha)b_2b_4 + \eta_1\alpha\varphi b_3)},\ \chi_{\gamma_H}^{\mathcal{R}_0} = -\frac{\gamma_H\alpha\eta_1\varphi b_3}{b_4\,(\alpha b_3 b_4 + \eta_2(1-\alpha)b_2b_4 + \eta_1\alpha\varphi b_3)}$$

$$\chi_\delta^{\mathcal{R}_0} = -\frac{\delta\alpha\eta_1\varphi b_3}{b_4\,(\alpha b_3 b_4 + \eta_2(1-\alpha)b_2b_4 + \eta_1\alpha\varphi b_3)},\ \chi_\varphi^{\mathcal{R}_0} = -\frac{\varphi\,(\alpha b_3 b_4 - \eta_1\alpha b_2 b_3 + \eta_1\alpha\varphi b_3)}{b_2\,(\alpha b_3 b_4 + \eta_2(1-\alpha)b_2b_4 + \eta_1\alpha\varphi b_3)},$$

$$\chi_\mu^{\mathcal{R}_0} = -\mu\left(\frac{1}{b_1} + \frac{\alpha b_3^2 b_4^2 + \eta_2(1-\alpha)b_2^2b_4^2 + \eta_1\alpha\varphi b_3^2(b_2+b_3)}{b_2b_3b_4\,(\alpha b_3 b_4 + \eta_2(1-\alpha)b_2b_4 + \eta_1\alpha\varphi b_3)}\right),\ \chi_{\eta_2}^{\mathcal{R}_0} = \frac{\eta_2(1-\alpha)b_2b_4}{\alpha b_3 b_4 + \eta_2(1-\alpha)b_2b_4 + \eta_1\alpha\varphi b_3}.$$

In Fig. 2, each one of parameters' impact on the basic reproduction number is shown. Indeed, Λ and ω do not appear in the expression of $\mathcal{R}_0$, therefore there is no sensitivity index related to them. After making the local sensitivity analysis, we noticed that the transmission rate β and the efficiency rate of the media coverage M are more influential in increasing and decreasing the reproduction number, respectively. However, $\chi_\beta^{\mathcal{R}_0} = +1$ that is 1% increase in β leads to an increase of 1% in $\mathcal{R}_0$. For $M = 50\%$, $\chi_M^{\mathcal{R}_0} = -1$ meaning that 1% increase in M leads to 1% decrease in $\mathcal{R}_0$. Similarly, $\chi_\alpha^{\mathcal{R}_0} = 0.2158$ expressing that 1% increase in α will induce 0.2158% increase in $\mathcal{R}_0$, and $\chi_\varphi^{\mathcal{R}_0} = -0.1499$ means that 1% increase in φ will produce 0.1499% decrease in $\mathcal{R}_0$. The same interpretation can be made for the rest of the parameters that appeared in the expression of $\mathcal{R}_0$ [7,8,39].

4.2. Herd immunity threshold computation

The course of a communicable disease can be slowed down or the spread of the disease can be somewhat blocked in an area when a certain rate of people recover from the disease with permanent immunity. In such situations, even though few people are still vulnerable, susceptible people are now rare in the population. This phenomenon called group immunity or herd immunity represents some kind of indirect protection for susceptible people due to their scarcity. In that case, if new infections do occur, isolation or containment strategy is easier to apply, [25,26]. However, the herd immunity threshold is related to the basic reproduction number and it can be computed as follows:

$$\frac{\mathcal{R}_0 - 1}{\mathcal{R}_0} = 1 - \frac{1}{\mathcal{R}_0}.$$

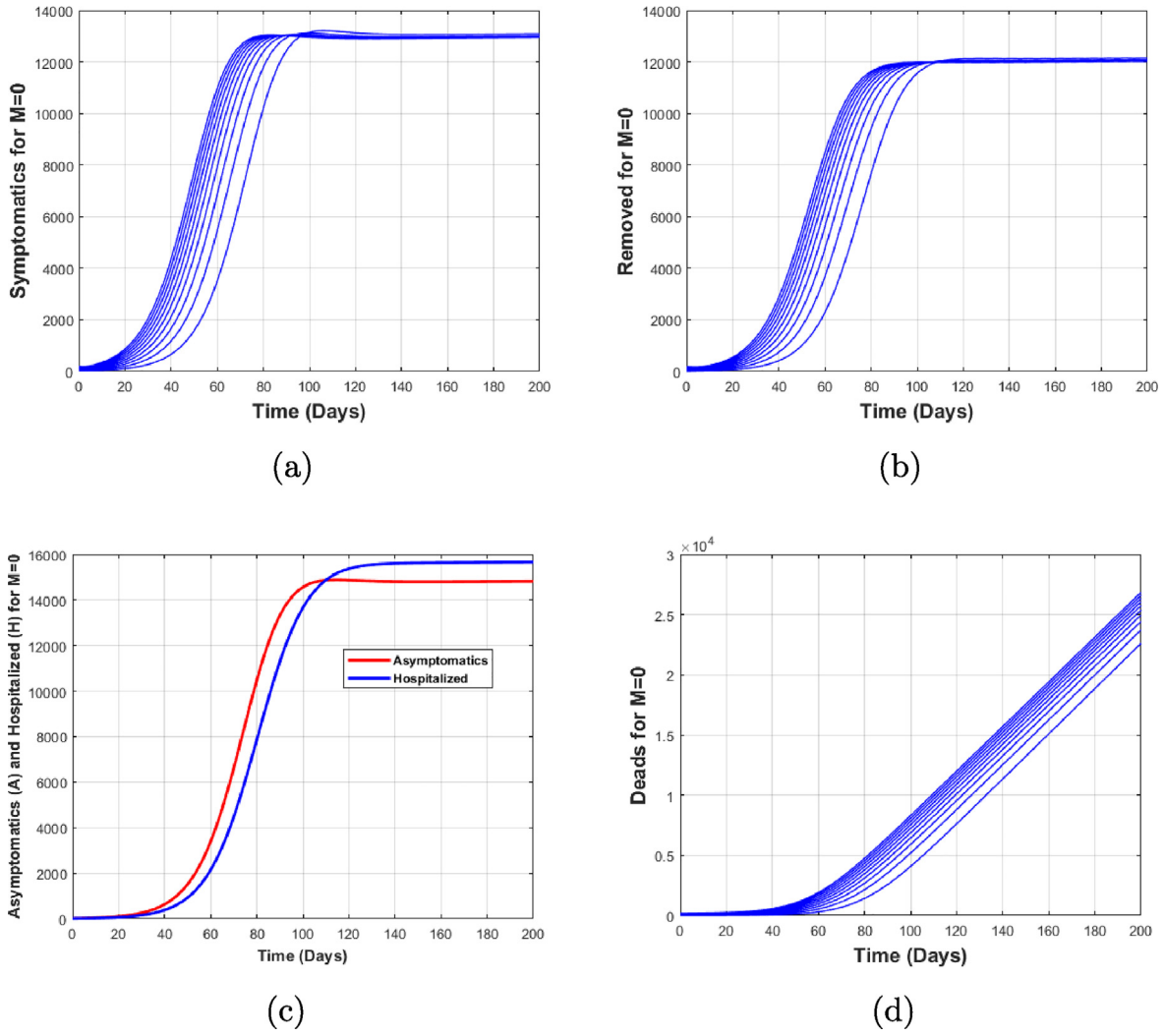

Fig. 3. Subfigures (a)–(d) describe the global dynamics of the disease when the media coverage has no effect on people behaviors at all. For this first case, $\mathcal{R}_0 \simeq 2.45$.

Indeed, it represents the proportion of the population that needs to be infected to reach the group immunity level. Moreover, from the above formula one can see that larger the value of $\mathcal{R}_0$, the faster herd immunity will occur [18,25]. Thus, after $(1 - 1/\mathcal{R}_0)$ % of the total population is infected, the disease may eventually die out (at least temporarily) until the mixing structure of the population changes. In this study, by first using data from Table 1 and secondly by assuming that the media coverage has no efficiency ($M = 0$) leads to $\mathcal{R}_0 \simeq 2.45$; so herd immunity normally occurs when about 59% of the total population is infected [18,25,26].

5. Numerical simulation

Here, by using the parameters from Table 1 which have mostly been borrowed from the literature [18,20,53], we have performed some simulations in order to numerically illustrate our theoretical results. We have assessed the impact of media coverage on the disease transmission dynamics by simulating the followings eventualities: if the media coverage had no efficiency at all, if the rate of efficiency of the media coverage were average or intense within an endemic area. Therefore, the parameter values that have been used lead to $\mathcal{R}_0 \simeq 2.45$ when there is no media coverage impact.

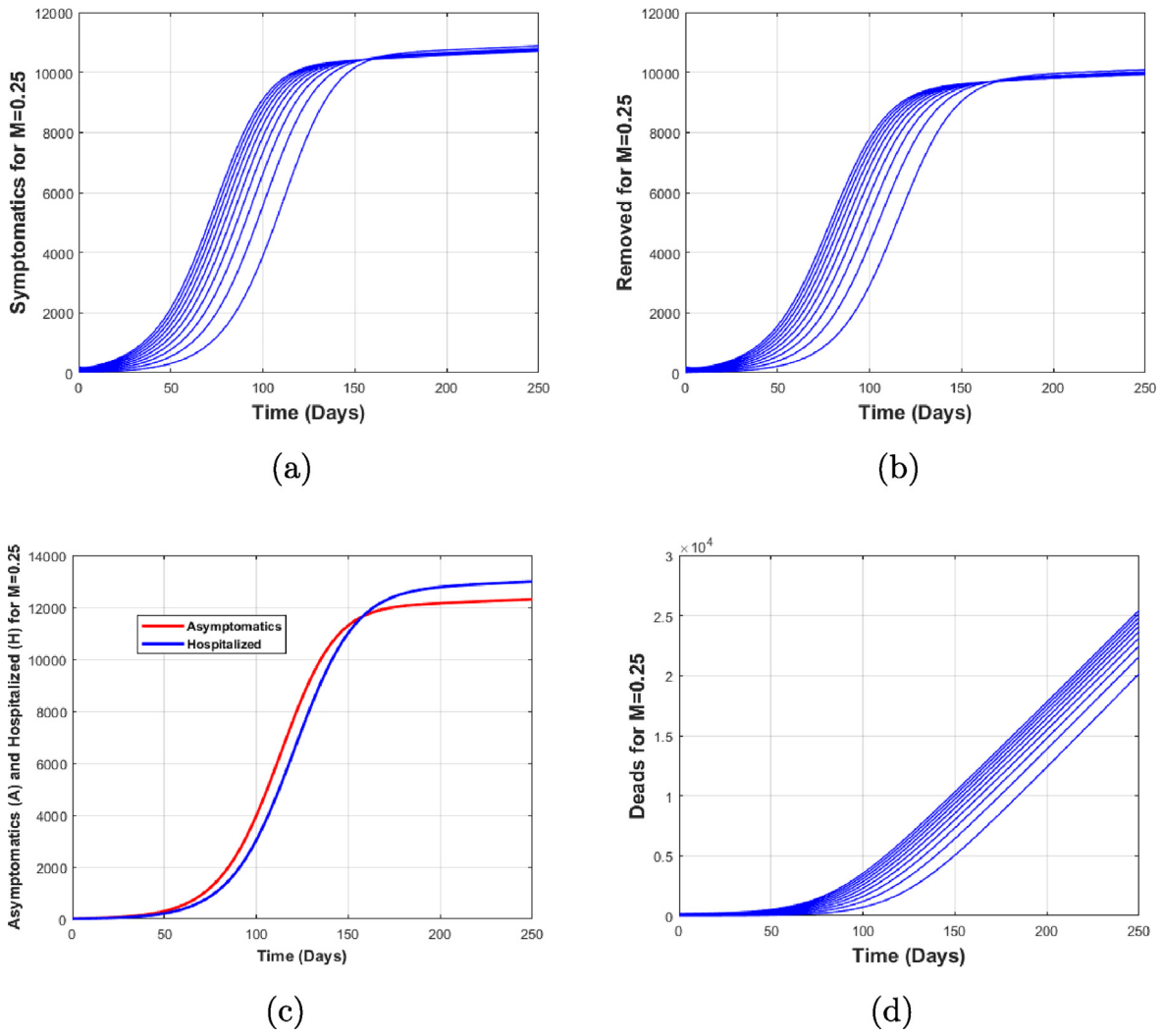

Fig. 4. Subfigures (a)–(d) describe the global dynamics of the disease when the media coverage efficiency rate is about 25%. We therefore have $\mathcal{R}_0 \simeq 1.84$.

From Figs. 3–7, in each of the subfigures (a), (b) and (d), we have presented the evolution of the population of the symptomatic individuals, recovered individuals, and dead persons, respectively by using various initial conditions. Besides, we have presented the evolution of asymptomatic individuals and hospitalized people all together in subfigure (c).

Fig. 3, 4 and 5 show the convergence of the solution of the system (2) towards endemic equilibrium when the rate of efficiency of the media coverage is zero, when it is 25% and when it is up to 50% respectively.

The simulation of model (2) by considering that the rate of efficiency of the media coverage is 67% and when it is about 75%, gives Figs. 6 and 7 respectively, which illustrate a convergence of the solution of this model towards the disease-free equilibrium.

Fig. 8, 9 and 10 are obtained by plotting in $3D$ the evolution of the different threshold parameters of the model, namely $\mathcal{R}_I$, $\mathcal{R}_A$, $\mathcal{R}_H$ and $\mathcal{R}_0$ when we have 25%, 50% and 75% as media coverage efficiency respectively.

Our numerical results show that the introduction of media coverage has trivial changes on the course of the disease relative to our baseline model. More precisely, an increase of the efficiency rate of the media coverage slows down the disease spreading dynamics. Moreover, we have noticed from our different scenarios of simulation that within an adequate environment, the disease extinction will occur when the media coverage efficiency exceeds

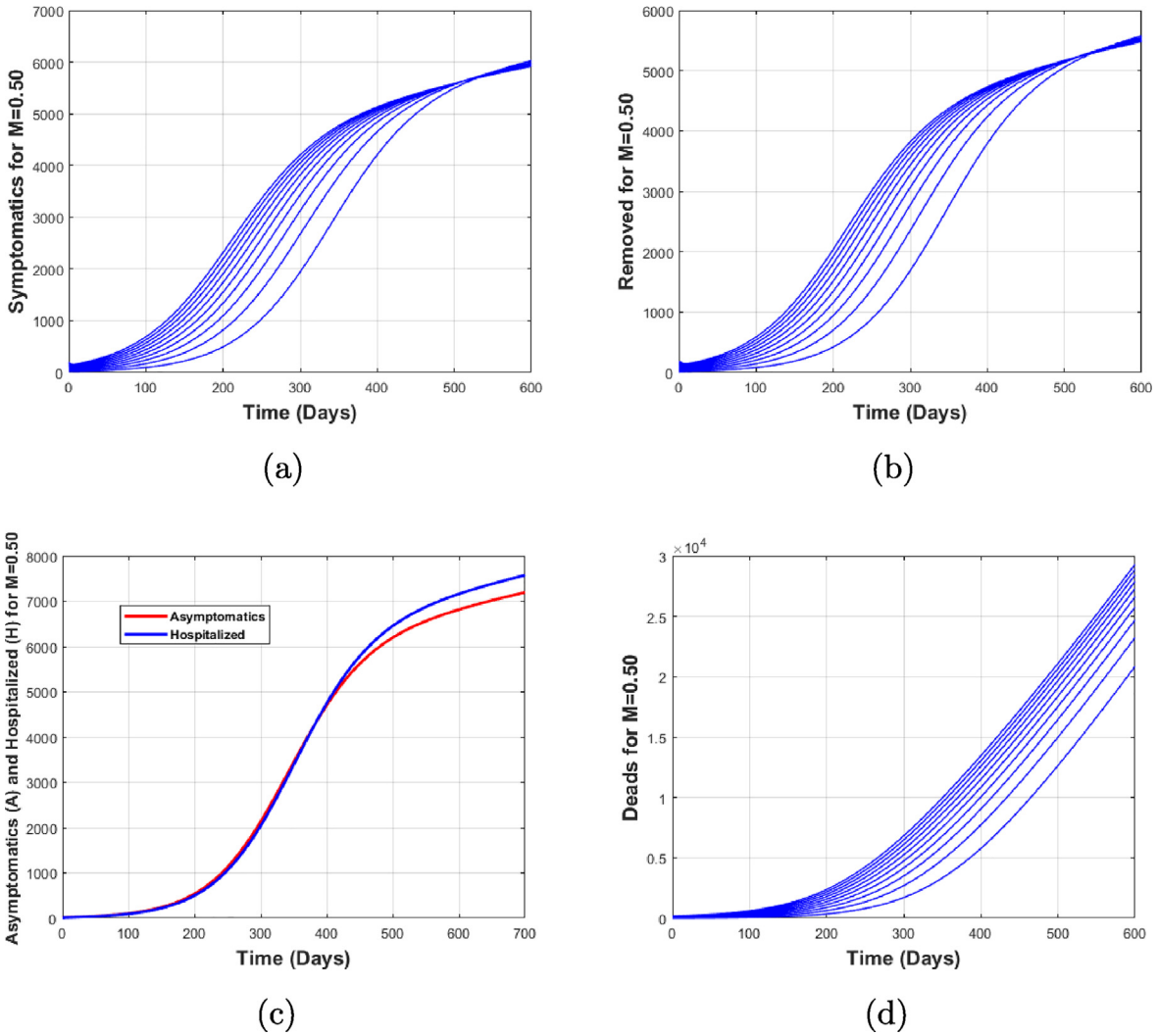

Fig. 5. Global dynamics of the disease when the efficiency rate of media coverage is up to 50%. In this case, we obtain $\mathcal{R}_0 \simeq 1.22$.

a threshold value $M \in]59\%, 60\%[$. Therefore, media coverage is a good strategy to control the outbreak of the current pandemic of the COVID-19, (see Figs. 3–7).

6. Conclusion and recommendations

In this manuscript, we have constructed and studied a deterministic compartmental mathematical model by considering the media coverage as a control strategy of the current pandemic of COVID-19 that is troubling the whole world [18,24,37]. Our modeling process first began with the study of some biological aspects of the disease that enabled us to better approach the modeling problem [13,25,44]. Mathematical analysis of the model shows that the course of the disease is governed by the basic reproduction number $\mathcal{R}_0$. Indeed, when $\mathcal{R}_0 < 1$ the disease disappears from the population giving a disease-free equilibrium which has been proved to be locally and globally asymptotically stable. Moreover, when $\mathcal{R}_0$ exceeds 1, the disease persists and leads to an endemic state which is also locally and globally asymptotically stable [12,17,55,57]. The sensitivity analysis of $\mathcal{R}_0$ shows how the different parameter variations will affect the disease dynamics [7,8,61]. In addition, computing herd immunity threshold parameter $(1 - 1/\mathcal{R}_0)$ % for $\mathcal{R}_0 \simeq 2.45$ when no control strategy is undertaken shows that a certain group immunity occurs when about 59% of the population is infected. There is then low transmission of the disease from this point

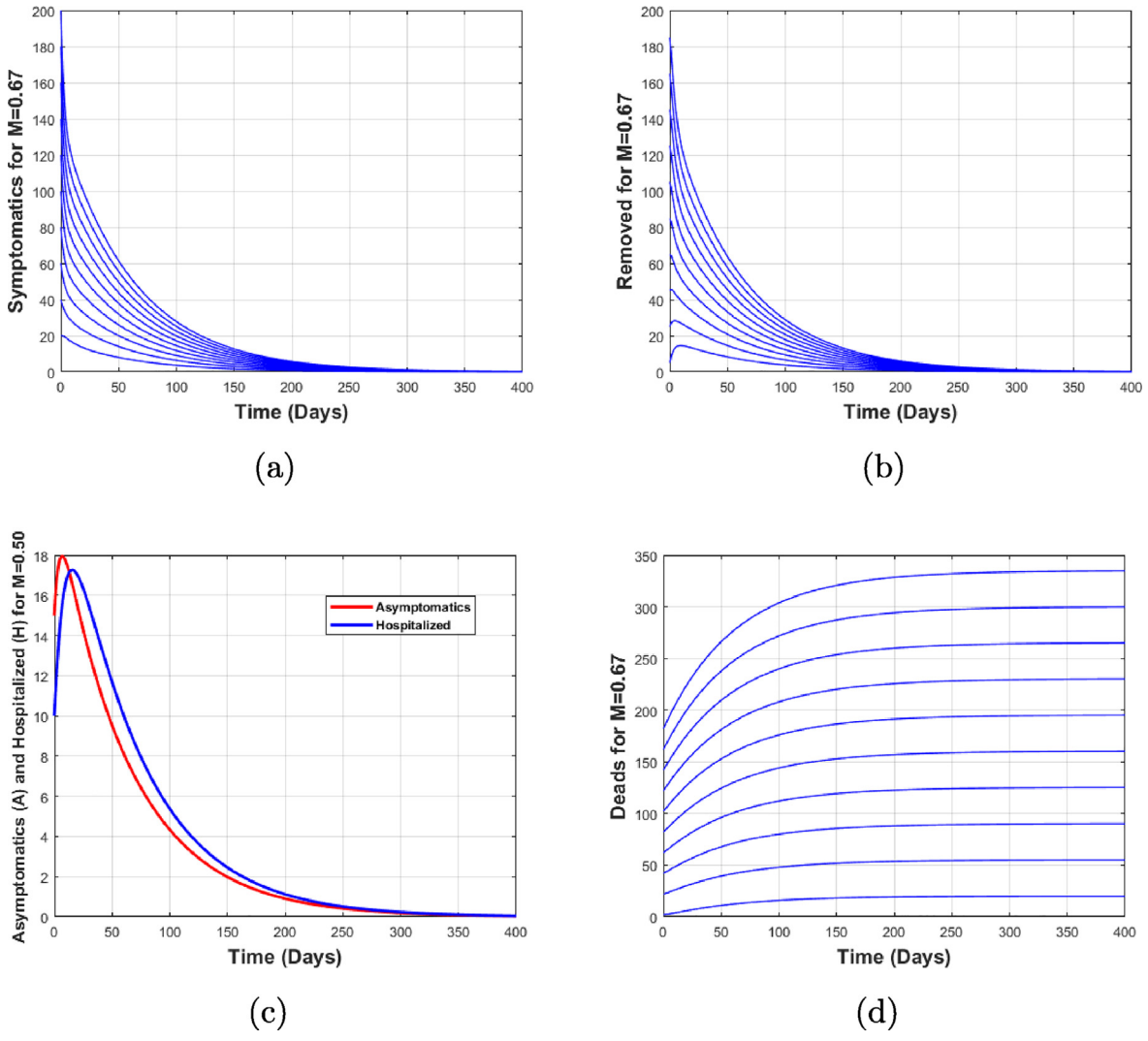

Fig. 6. Global dynamics of the disease when the rate of efficiency of the media coverage is up to 67%. So, $\mathcal{R}_0 \simeq 0.81$.

on [25,26,39]. We used different scenarios for the model simulation and the results have shown that being aware and respecting safety guidelines such as wearing of masks, social distancing, frequent disinfection of hands with water and soap or using any other means to keep from being infected and cutting down as much as possible on travel has positive effect in the combat against the coronavirus rapid spread [13,40,62]. The course of a pandemic is determined by individual and collective actions of people, who internalize the information available to them such as the severity, mortality, and modes of transmission of the disease [8,18,26,58]. Such information enhance the public adherence to the government interventions, policies and directives so that to achieve the expected results. Therefore, a large campaign of education through media coverage may play a crucial role in the fight against the ongoing pandemic of COVID-19 [1,2,37].

In this study, the model is formulated by using ordinary differential equations. However, it has been proven that the use of fractional derivatives gives more realistic description of most biological issues compared to ordinary derivatives. Therefore, for future investigations, it will be interesting to consider fractional derivative while formulating a COVID-19 transmission model that would give a better description of the biological process [1–3,9, 51].

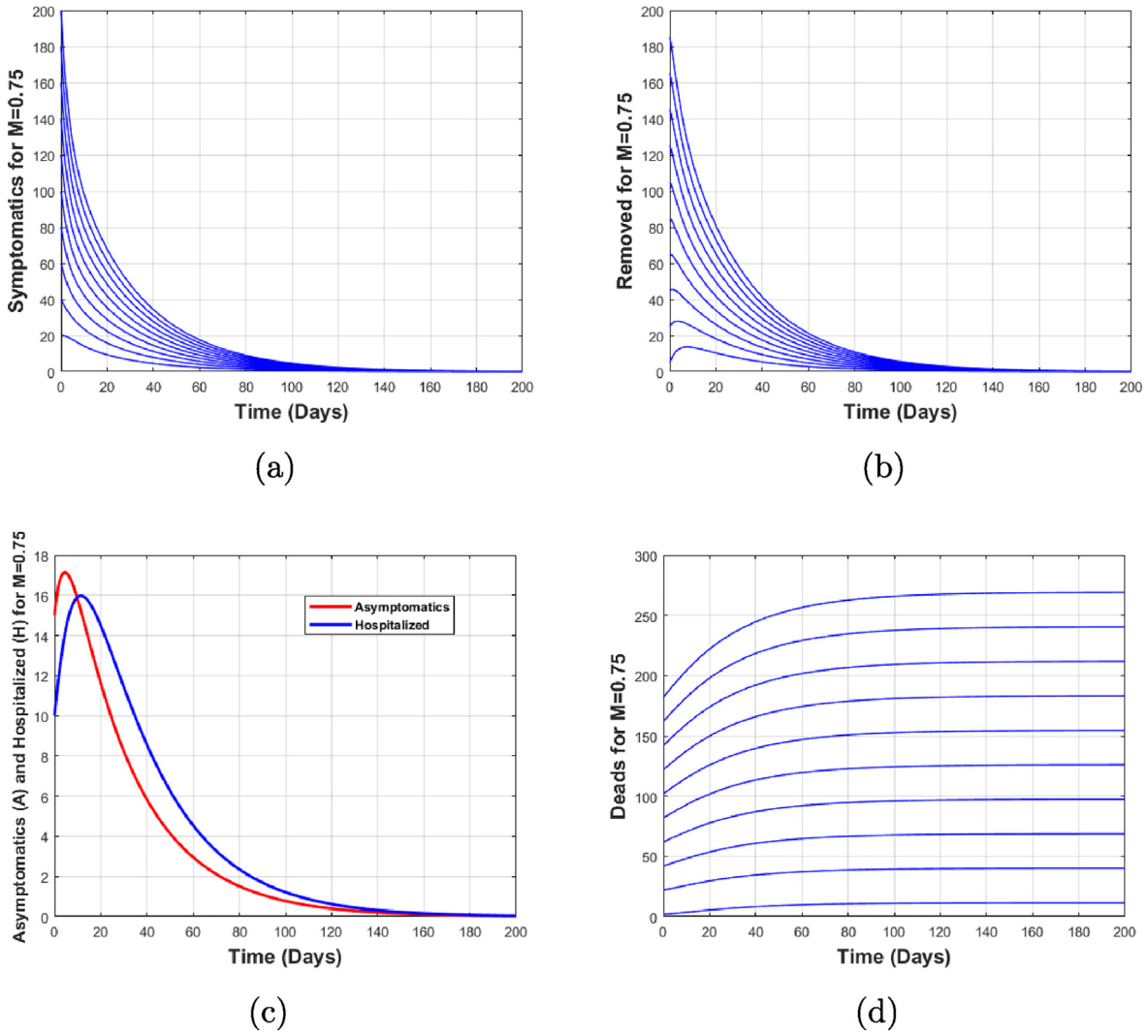

Fig. 7. Subfigures (a)–(d) present the global dynamics of the disease when the media coverage efficiency rate reaches $M = 75\%$, such that $\mathcal{R}_0 \simeq 0.61$.

Declaration of competing interest

The authors declare that they have no known competing financial interests or personal relationships that could have appeared to influence the work reported in this paper.

Acknowledgments

The authors are immensely grateful to the associate editor and the anonymous referees for their constructive comments on an earlier version of the manuscript and suggestions given in their reports, which have helped us to significantly polish this work.

The authors are very much thankful to the Erasmus+ Mobility Program and more especially to Prof. Matias Raja, coordinator of Erasmus+ Mobility Program at the University of Murcia (Spain).

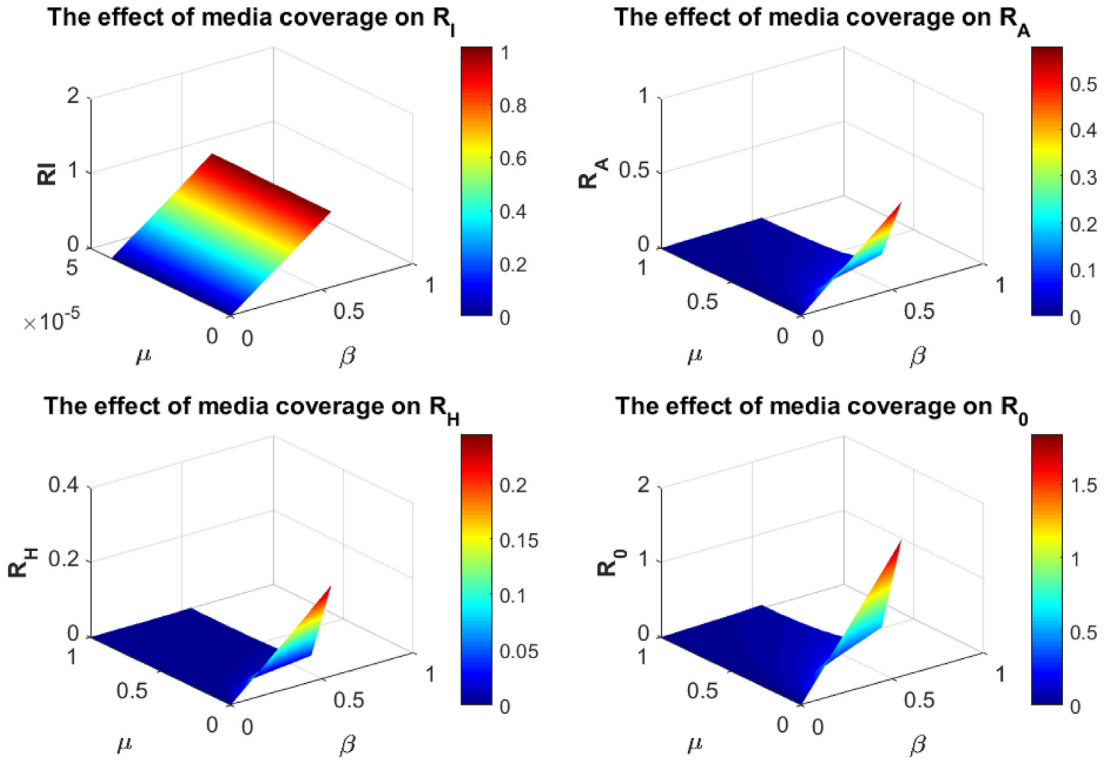

Fig. 8. Evolution of the threshold parameters when the efficiency rate of the media coverage is $M = 25\%$.

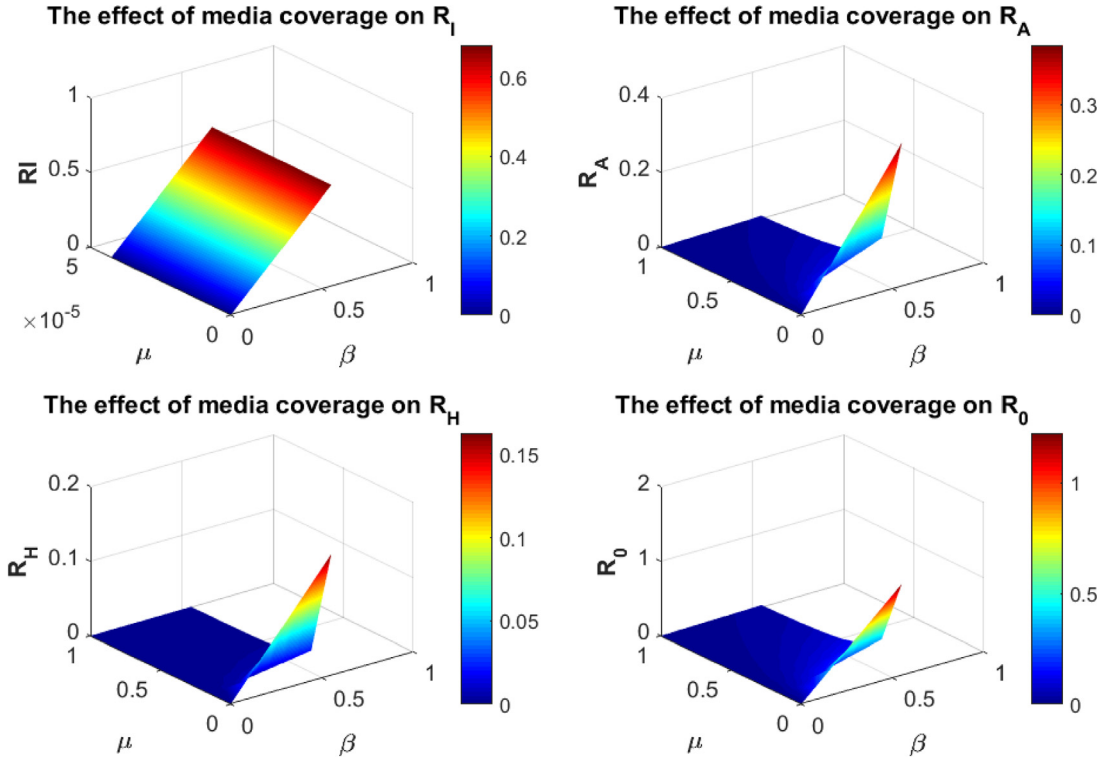

Fig. 9. Evolution of the threshold parameters when the efficiency rate of the media coverage is $M = 50\%$.

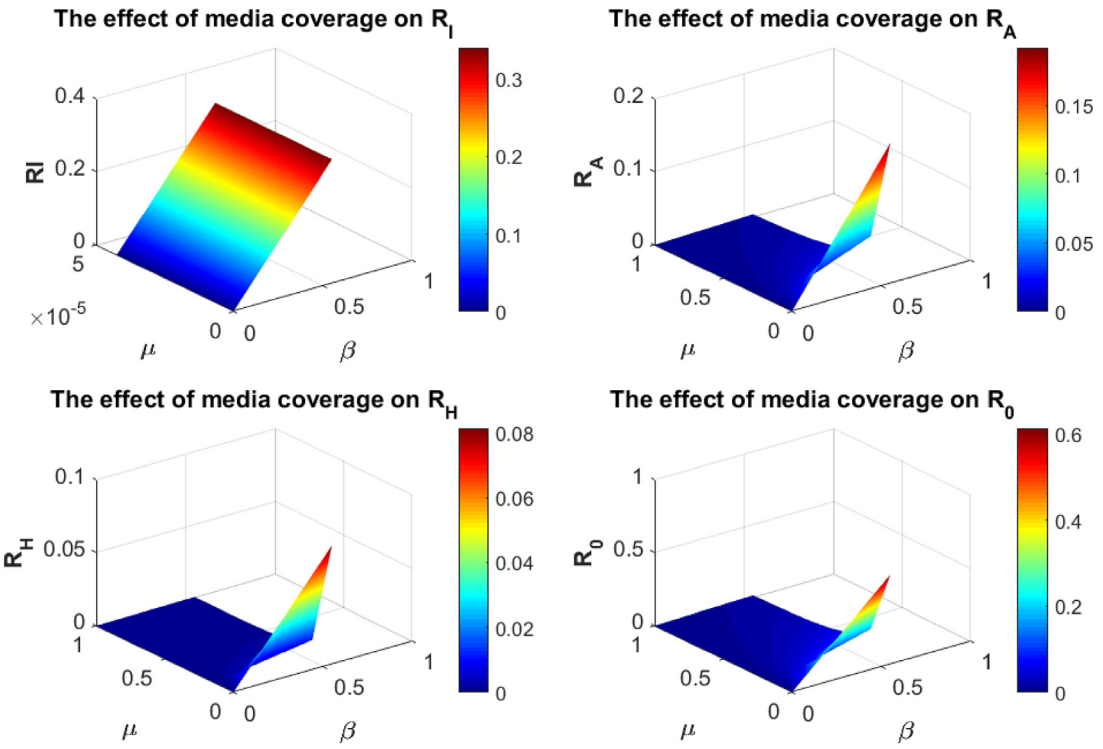

Fig. 10. Evolution of the threshold parameters when the efficiency rate of the media coverage is $M = 75\%$.

Table 1
Model parameters values and sensitivity indices.

Parameters	Values	References	Dimensions	Sensitivity indices
Λ	200	estimated	humans/day	–
ω	0.42	estimated	/day	–
β	0.55	[18,36]	/day	+1
η_1	0.2	[18,53]	–	+0.1327
η_2	0.5	[20,36]	–	+0.3137
σ	1/6	[18,36]	/day	+0.00025
α	0.6	[20,36]	–	+0.2158
φ	0.1	[20,64]	/day	−0.1499
γ_A	1/7	[53,64]	/day	−0.3136
γ_I	1/7	[53,64]	/day	−0.4036
γ_H	1/14	[53,64]	/day	−0.1135
μ	4.25×10^{-5}	estimated	/day	−0.00055
δ	0.012	[18,20]	/day	−0.0191
M	50%	estimated	–	−1

References

[1] https://link.springer.com/chapter/10.1007/978-981-16-2450-6.
[2] S. Ahmad, A. Ullah, Q.M. Al-Mdallal, H. Khan, K. Shah, A. Khan, Fractional order mathematical modeling of COVID-19 transmission, Chaos Solitons Fractals 139 (110256) (2020).
[3] M. Al-Refai, On weighted Atangana-Baleanu fractional operators, Adv. Differential Equations 2020 (3) (2020).
[4] M. Ali, S.T.H. Shah, M. Imran, A. Khan, The role of asymptomatic class, quarantine and isolation in the transmission of COVID-19, J. Biol. Dyn. 14 (1) (2020) 389–408.
[5] R.M. Anderson, R.M. May, Infectious Diseases of Humans: Dynamics and Control, Oxford University Press, Oxford, 1991.
[6] J. Arino, S. Portet, A simple model for COVID-19, Infect. Dis. Model. 5 (2020) 309–315.
[7] J.K.K. Asamoah, Z. Jin, G.-Q. Sun, Non-seasonal and seasonal relapse model for Q fever disease with comprehensive cost-effectiveness analysis, Results Phys. 22 (103889) (2021).

[8] J.K.K. Asamoah, M.A. Owusu, Z. Jin, F.T. Oduro, A. Abidemi, E.O. Gyasi, Global stability and cost-effectiveness analysis of COVID-19 considering the impact of the environment: using data from Ghana, Chaos Solitons Fractals 140 (110103) (2020).
[9] A. Atangana, D. Baleanu, A new fractional derivatives with nonlocal and non-singular kernel: theory and application to heat tranfer model, Term. Sci. 20 (2) (2016) 763–769.
[10] R. Bellman, K.L. Cooke, Differential-Difference Equations, Academic Press, New York and London, 1963.
[11] J.C. Blackwood, L.M. Childs, An introduction to compartmental modeling for the budding infectious disease modeler, Lett. Biomath. 5 (1) (2018) 195–221.
[12] F. Brauer, Mathematical epidemiology: Past, present, and future, Infect. Dis. Model. 2 (2) (2017) 113–127.
[13] X. Chen, B. Yu, First two months of the 2019 coronavirus disease (COVID-19) epidemic in China: Real-time surveillance and evaluation with a second derivative model, Glob. Health Res. Policy 5 (7) (2020).
[14] C. Connell McCluskey, Global stability of an SIR epidemic model with delay and general nonlinear incidence, Math. Biosci. Eng. 7 (4) (2010) 837–850.
[15] R.M. Cotta, C.P. Naveira-Cotta, P. Magal, Mathematical parameters of the COVID-19 epidemic in Brazil and evaluation of the impact of different public health measures, Biology 9 (220) (2020).
[16] J. Demongeot, Q. Q. Griette, P. Magal, SI epidemic model applied to COVID-19 data in mainland China, R. Soc. Open Sci. 7 (201878) (2020).
[17] O. Diekmann, J.A.P. Heesterbeek, J.A.J. Metz, On the definition and the computation of the basic reproduction ratio R0 in models for infectious diseases in heterogeneous populations, J. Math. Biol. 28 (4) (1990) 365–382.
[18] S.E. Eikenberry, M. Mancuso, E. Iboi, T. Phan, K. Eikenberry, Y. Kuang, E. Kostelich, A.B. Gumel, To mask or not to mask: Modeling the potential for face mask use by the general public to curtail the COVID-19 pandemic, Infect. Dis. Model. 5 (2020) 293–308.
[19] L.X. Feng, S.L. Jing, S.K. Hu, D.F. Wang, H.F. Huo, Modelling the effects of media coverage and quarantine on the COVID-19 infections in the UK, Math. Biosci. Eng. 17 (4) (2020) 3618–3636.
[20] N. Ferguson, D. Laydon, G. Nedjati Gilani, N. Imai, K. Ainslie, M. Baguelin, et al., Report 9: Impact of non-pharmaceutical interventions (NPIs) to reduce COVID-19 mortality and healthcare demand, 2020.
[21] A. Guiro, S. Ouaro, A. Traoré, Stability analysis of a schistosomiasis model with delays, Adv. Differential Equations 303 (2013).
[22] J.K. Hale, S.M.V. Lunel, Introduction to functional differential equations, Appl. Math. Sci. 99 (1993).
[23] H.W. Hethcote, The mathematics of infectious diseases, SIAM Rev. 42 (4) (2000) 599–653.
[24] B. Ivorra, M.R. Ferrández, M. Vela-Pérez, A.M. Ramos, Mathematical modeling of the spread of the coronavirus disease 2019 (COVID-19) taking into account the undetected infections, Case China. Commun. Nonlinear Sci. Numer. Simul. 88 (105303) (2020).
[25] S.M. Kassa, J.B.H. Njagarah, Y.A. Terefe, Modelling Covid-19 mitigation and control strategies in the presence of migration and vaccination: the case of South Africa, Afr. Mat. (2021).
[26] S.M. Kassa, J.B.H. Njagaraha, Y.A. Terefe, Analysis of the mitigation strategies for COVID-19: From mathematical modelling perspective, Chaos Solitons Fractals 138 (109968) (2020).
[27] S.M. Kassa, Y.H. Workineh, Effect of negligence and length of time delay in spontaneous behavioural changes for the response to epidemics, Math. Methods Appl. Sci. 41 (18) (2018) 8613–8635.
[28] W.O. Kermack, A.G. McKendrick, A contribution to the mathematical theory of epidemics, Proc. R. Soc. Lond. Ser. A Math. Phys. Eng. Sci. 115 (1927) 700–721.
[29] A. Korobeinikov, Lyapunov functions and global stability for SIR and SIRS epidemiological models with non-linear transmission, Bull. Math. Biol. 68 (3) (2006) 615–626.
[30] O. Koutou, B. Sangaré, A.B. Diabaté, Mathematical analysis of mosquito population global dynamics using delayed-logistic growth, Malaya J. Mat. 8 (4) (2020) 1898–1905.
[31] O. Koutou, B. Traoré, B. Sangaré, Mathematical model of malaria transmission dynamics with distributed delay and a wide class of nonlinear incidence rates, Cogent Math. Stat. 5 (1564531) (2018).
[32] O. Koutou, B. Traoré, B. Sangaré, Mathematical modeling of malaria transmission global dynamics: taking into account the immature stages of the vectors, Adv. Differential Equations 2018 (220) (2018).
[33] S. Kumar, C. Xu, N. Ghildayal, C. Chandra, M. Yang, Social media effectiveness as a humanitarian response to mitigate influenza epidemic and COVID-19 pandemic, Ann. Oper. Res. (2021) 1–29.
[34] V. Lakshmikantham, S. Leela, A.A. Martynyuk, Stability Analysis of Nonlinear Systems, Marcel Dekker, New York, 1989.
[35] J.P. LaSalle, The Stability of Dynamical Systems, SIAM, Philadelphia, 1976.
[36] R. Li, S. Pei, B. Chen, Y. Song, T. Zhang, W. Yang, et al., Substantial undocumented infection facilitates the rapid dissemination of novel coronavirus (SARS-CoV2), Science (2020).
[37] N. Liu, Z. Chen, G. Bao, Role of media coverage in mitigating COVID-19 transmission: Evidence from China, Technol. Forecast. Soc. Change 163 (120435) (2021).
[38] Z. Liu, P. Magal, O. Seydi, Glenn Webb, Predicting the cumulative number of cases for the COVID-19 epidemic in China from early data, MBE 17 (4) (2020).
[39] A.M. Lutambi, M.A. Penny, T. Smith, N. Chitnis, Mathematical modelling of mosquito dispersal in a heterogeneous environment, Math. Biosci. 241 (2) (2013) 198–216.
[40] P. Magal, A COVID-19 epidemic model with latency period, 2020, Available at SSRN: https://ssrn.com/abstract3558797.
[41] M. Mahrouf, A. Boukhouima, H. Zine, E.M. Lotfi, D.F.M. Torres, N. Yousfi, Modeling and forecasting of COVID-19 spreading by delayed stochastic differential equations, Axioms 10 (1) (2021).
[42] P. Manfredi, A. d'Onofrio (Eds.), Modeling the Interplay Between Human Behavior and the Spread of Infectious Diseases, Springer, New York, 2013.

[43] J. Mushanyu, Z. Chazuka, F. Mudzingwa, C. Ogbogbo, Modelling the impact of detection on COVID-19 transmission dynamics in Ghana, Res. Math. Stat. 8 (1) (2021).
[44] F. Ndaïrou, I. Area, J.J. Nieto, D.F.M. Torres, Mathematical modeling of COVID-19 transmission dynamics with a case study of Wuhan, Chaos Solitons Fractals 135 (109846) (2020).
[45] J. Norton, An introduction to sensitivity assessment of simulation models, Environ. Model. Softw. 69 (2015) 166–174.
[46] L.L. Obsu, S.F. Balcha, Optimal control strategies for the transmission risk of COVID-19, J. Biol. Dyn. 14 (1) (2020) 590–607.
[47] H. Ouedraogo, W. Ouedraogo, B. Sangaré, A self-diffusion mathematical model to describe the Toxin effect on the Zooplankton dynamics, Nonlinear Dyn. Syst. Theory 18 (4) (2018) 392–408.
[48] R. Padmanabhan, H.S. Abed, N. Meskin, T. Khattab, M. Shraim, M.A. Al-Hitmi, A review of mathematical model-based scenario analysis and interventions for COVID-19, Comput. Methods Programs Biomed. 209 (106301) (2021).
[49] R.K. Rai, S. Khajanchi, P.K. Tiwari, E. Venturino, A.K. Misra, Impact of social media advertisements on the transmission dynamics of COVID-19 pandemic in India, J. Appl. Math. Comput. (2021) p1–26.
[50] Q. Richard, S. Alizon, M. Choisy, M.T. Sofonea, R. Djidjou-Demasse, Age-structured non-pharmaceutical interventions for optimal control of COVID-19 epidemic, PLoS Comput. Biol. 17 (3) (2021).
[51] Q. Richard, M. Choisy, T. Lefèvre, R. Djidjou-Demasse, Human-vector malaria transmission model structured by age, time since infection and waning immunity, Nonlinear Anal. RWA 63 (1) (2021).
[52] A. Savadogo, B. Sangaré, H. Ouedraogo, A mathematical analysis of Hopf-bifurcation in a prey-predator model with nonlinear functional response, Adv. Differential Equations 2021 (275) (2021).
[53] B. Tang, N.L. Bragazzi, Q. Li, S. Tang, Y. Xiao, J. Wu, An updated estimation of the risk of transmission of the novel coronavirus (2019-ncov), Infect. Dis. Model. 5 (2020) 248–255.
[54] B. Traoré, O. Koutou, B. Sangaré, Global dynamics of a seasonal mathematical model of schistosomiasis transmission with general incidence function, J. Biol. Syst. 27 (1) (2019) 19–49.
[55] B. Traoré, O. Koutou, B. Sangaré, A global mathematical model of malaria transmission dynamics with structured mosquito population and temperature variations, Nonlinear Anal. RWA 53 (103081) (2020).
[56] S. Tyagi, S.C. Martha, S. Abbas, A. Debbouche, Mathematical modeling and analysis for controlling the spread of infectious diseases, Chaos Solitons Fractals 144 (110707) (2021) 1–15.
[57] P. van den Driessche, J. Watmough, Reproduction numbers and sub-threshold endemic equilibria for compartmental models of disease transmission, Math. Biosci. 180 (2002) 29–48.
[58] Z. Wang, C.T. Bauch, S. Bhattacharyya, A. d'Onofrio, P. Manfredi, M. Perc, N. Perra, M. Salathé, D. Zhao, Statistical physics of vaccination, Phys. Rep. 664 (2016) 1–113.
[59] Q. Yan, Y. Tang, D. Yan, J. Wang, L. Yang, X. Yang, S. Tang, Impact of media reports on the early spread of COVID-19 epidemic, J. Theoret. Biol. 502 (2020).
[60] C. Yang, J. Wang, A mathematical model for the novel coronavirus epidemic in Wuhan, China, Math. Biosci. Eng. 17 (3) (2020) 2708–2724.
[61] M. Youcef, A reaction–diffusion system to better comprehend the unlockdown: Application of SEIR-type model with diffusion to the spatial spread of COVID-19 in France, Comput. Math. Biophys. 2020 (8) (2020) 102–113.
[62] A. Zeb, E. Alzahrani, V.S. Erturk, G. Zaman, Mathematical Model for Coronavirus Disease 2019 (COVID-19) Containing Isolation Class, Vol. 2020, BioMed Research International PB, Hindawi, 2020, 3452402, 7.
[63] W.K. Zhou, A.L. Wang, F. Xia, Y.N. Xiao, S.Y. Tang, Effects of media reporting on mitigating spread of COVID-19 in the early phase of the outbreak, Math. Biosci. Eng. 17 (3) (2020) 2693–2707.
[64] F. Zhou, T. Yu, R. Du, G. Fan, Y. Liu, Z. Liu, et al., Clinical course and risk factors for mortality of adult inpatients with COVID-19 in Wuhan, China: A retrospective cohort study, Lancet 395 (2020) 1054–1062.
[65] H. Zine, A. Boukhouima, E.M. Lotfi, M. Mahrouf, D.F.M. Torres, N. Yousfi, A stochastic time-delayed model for the effectiveness of Moroccan COVID-19 deconfinement strategy, Math. Model. Nat. Phenom. 15 (50) (2020) 1–14.